ARMY RESEARCH LABORATORY

The Impact of Aerosols and Battlefield Obscurants on Ultrashort Laser Pulse Propagation

by Chase A. Munson and Anthony R. Valenzuela

ARL-TR-5834 **December 2011**

NOTICES

Disclaimers

The findings in this report are not to be construed as an official Department of the Army position unless so designated by other authorized documents.

Citation of manufacturer's or trade names does not constitute an official endorsement or approval of the use thereof.

Destroy this report when it is no longer needed. Do not return it to the originator.

Army Research Laboratory
Aberdeen Proving Ground, MD 21005-5066

ARL-TR-5834 **December 2011**

The Impact of Aerosols and Battlefield Obscurants on Ultrashort Laser Pulse Propagation

Chase A. Munson and Anthony R. Valenzuela
Weapons and Materials Research Directorate, ARL

REPORT DOCUMENTATION PAGE	Form Approved OMB No. 0704-0188

1. REPORT DATE *(DD-MM-YYYY)*	2. REPORT TYPE	3. DATES COVERED (From - To)
December 2011	Final	1 October 2010–30 September 2011

4. TITLE AND SUBTITLE
The Impact of Aerosols and Battlefield Obscurants on Ultrashort Laser Pulse Propagation

5a. CONTRACT NUMBER

5b. GRANT NUMBER

5c. PROGRAM ELEMENT NUMBER

6. AUTHOR(S)
Chase A. Munson and Anthony R. Valenzuela

5d. PROJECT NUMBER
FASLW-2a-2011

5e. TASK NUMBER

5f. WORK UNIT NUMBER

7. PERFORMING ORGANIZATION NAME(S) AND ADDRESS(ES)
U.S. Army Research Laboratory
ATTN: RDRL-WML-A
Aberdeen Proving Ground, MD 21005-5066

8. PERFORMING ORGANIZATION REPORT NUMBER
ARL-TR-5834

9. SPONSORING/MONITORING AGENCY NAME(S) AND ADDRESS(ES)

10. SPONSOR/MONITOR'S ACRONYM(S)

11. SPONSOR/MONITOR'S REPORT NUMBER(S)

12. DISTRIBUTION/AVAILABILITY STATEMENT
Approved for public release; distribution is unlimited.

13. SUPPLEMENTARY NOTES

14. ABSTRACT
Ultrashort pulsed laser propagation through the atmosphere has been studied by both theory and simulation and through laboratory experiments. At sufficiently high pulse energies (on the order of several gigawatts), propagating laser pulses become subject to various nonlinear optical effects, and optical phenomena known as laser filaments are produced. Applying ultrashort laser pulses and laser filaments in the battlefield environment requires a solid physical and theoretical understanding of how these pulses and filaments propagate through the air and interact with battlefield obscurants, such as diesel exhaust, smokes, and dust. Existing open literature on the topic has investigated only the impact of well-defined, aqueous aerosols on ultrashort laser pulses and filaments. In this report, we review the existing works on the topic, discuss where more fundamental scientific understanding is needed, and outline some of the challenges that need to be addressed to utilize the potential of ultrashort laser pulses on the battlefield.

15. SUBJECT TERMS
ultrashort pulsed lasers, filamentation, aerosols, obscurants

16. SECURITY CLASSIFICATION OF:			17. LIMITATION OF ABSTRACT	18. NUMBER OF PAGES	19a. NAME OF RESPONSIBLE PERSON
a. REPORT	b. ABSTRACT	c. THIS PAGE			Chase A. Munson
Unclassified	Unclassified	Unclassified	UU	44	19b. TELEPHONE NUMBER (*Include area code*) (410) 278-1369

Standard Form 298 (Rev. 8/98)
Prescribed by ANSI Std. Z39.18

Contents

List of Figures

1. Introduction

Temporally short laser pulses on the order of hundreds of femtoseconds in duration, such as those produced by ultrashort pulsed laser (USPL) systems, under certain conditions will produce intense channels of light known as filaments when propagated through the atmosphere (*1*). The physical processes underlying filament formation and atmospheric propagation, as well as applications exploiting the unique properties of these filaments, has been an area of intense research since the mid-1990s and has been summarized in several reviews (*2–4*). Femtosecond filaments may be projected at distances approximately several kilometers and propagate hundreds of meters in air (*5*). In addition, upon termination, the filament produces a supercontinuum of white light (*6*, *7*). These filament properties make the process of filamentation an attractive tool for long-distance sensing applications. Filamentation has been proposed as a light source for light detecting and ranging (LIDAR), (*8*) and large-scale systems such as the Teramobile (*9*) have been developed to study filament propagation and LIDAR sensing. Filament-based detection has been investigated for toxic metallic vapors, (*10*) biological species, (*11*) and explosives (*12*).

The battlefield environment presents unique challenges for the use of lasers since propagation through these environments is complicated by many natural and manmade particulates. Diesel exhaust, dust, water vapor, and smoke all serve to scatter and absorb laser radiation, reducing the effectiveness of lasers as sensing and illumination tools. Experimental and theoretical studies of filaments have demonstrated the resistance of these filaments to disruption by aerosolized water droplets (*13–15*). Tailoring the properties of these filaments for sensing and illumination applications requires a fundamental understanding of how aerosols and airborne particulates impact filament propagation.

2. Scope of This Review

The formation and propagation of filaments through liquids and gases has been intensively studied through experiment and simulation (*2–4*). Despite these studies, many aspects of filament formation and propagation remain only partially understood. Complications in filament propagation due to atmospheric constituents such as particulates and aerosols, (*15–17*) as well disruption due to atmospheric turbulence (*18*), have been explored to a lesser extent. Most of these studies are aimed at understanding filament propagation in the presence of aqueous aerosols and encompass a broad scope: from experiment to simulation, single aerosol droplets to rainstorms, and laboratory studies to outdoor propagation in various environments (maritime, high and low altitude) at hundreds of meters. No open literature to date presents studies on the influence of solid airborne particulates, e.g., dust or soot, on filament structure and propagation.

This report provides a comprehensive review of experimental and theoretical studies related to ultrashort laser propagation through aerosols. We first briefly discuss the physical process of filamentation in air, followed by the experimental and theoretical investigations of filament propagation through aerosols. Last, we examine the challenges of using filaments for sensing and illumination beyond particulates found within complex environments, such as the battlefield.

3. Laser Pulse Filamentation in Air

Although the physics behind the formation of filaments in air has been studied intensely through experiment and simulation, it continues to be debated. The science of filamentation has been discussed in detail in the literature (*2–4*). In brief, the formation of filaments is principally governed by two nonlinear optical processes: the optical Kerr effect and plasma formation and defocusing. As ultrashort laser pulses of sufficient power propagate through the atmosphere, the optical Kerr effect causes slow self-focusing of the laser pulses, which overcomes the linear beam spread due to diffraction of the laser pulse. The required laser power for self-focusing, known as the critical power (P_{cr}), is defined by Marburger as (*19*)

$$P_{cr} \equiv \frac{3.72\lambda_0^2}{8\pi n_0 n_2}, \tag{1}$$

where n_0 is the linear refractive index, n_2 is the nonlinear Kerr index coefficient, and λ_0 is the wavelength of the laser source. For a typical Ti:Sapphire laser propagating through air, values of 800 nm, 1, and 3×10^{-19} cm^2/W are used for λ_0, n_0, and n_2, respectively. This results in a critical power requirement for Kerr self-focusing in air of ~3.3 GW. An additional study by Liu and Chin (*20*) indicates that the value of n_2 is disputed (experimental measurement and theory do not agree). Experimental techniques developed in their work produced pulse-length-dependent values of P_{cr} ranging from 5 GW (t_p = 200 fs) to 10 GW (t_p = 42 fs). Energy contained in the laser pulse is often reported as multiples of P_{cr} (e.g., 5 P_{cr} = 5 × P_{cr} = ~17–50 GW).

The second nonlinear effect required for filament formation is multiphoton ionization coupled with plasma defocusing. As Kerr self-focusing progresses, the laser pulse intensity increases, leading to photoionization of the air. This ionization of the air results in the formation of a plasma and a local change in the refractive index of the air, causing the air to behave as a divergent lens and the laser energy to defocus. In the regime above P_{cr} but below the relativistic regime of 10^{16} W/cm^2, the Kerr self-focusing and plasma defocusing successfully compete and form a stable column of plasma (~100–150 µm in diameter) known as a filament. At laser powers exceeding the relativistic regime boundary, plasma defocusing predominates over self-focusing, limiting the intensity available to form filaments. Figure 1 illustrates the roles of these competing processes in the formation of the laser filament.

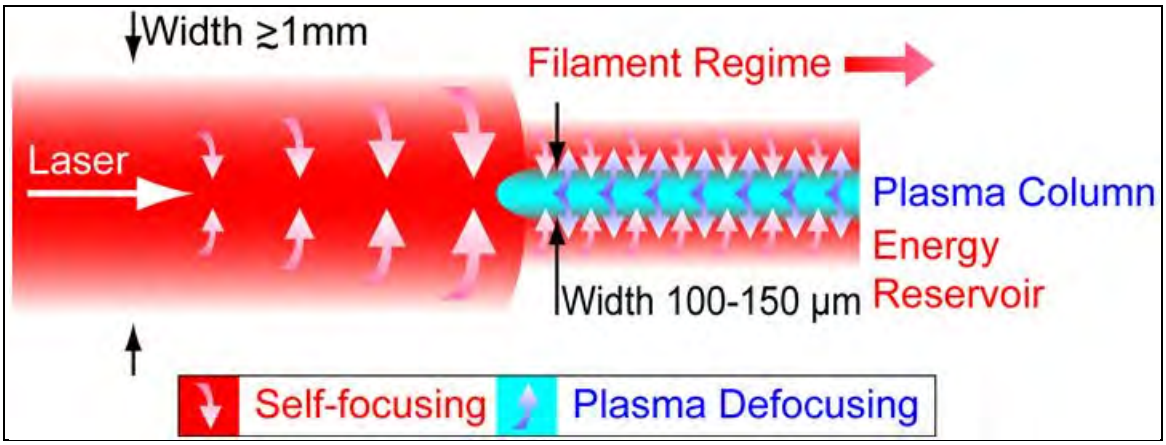

Figure 1. Nonlinear physical processes leading to the formation of a filament.

Propagation of the filament continues while sufficient laser energy remains in the region surrounding the filament (energy reservoir) to drive the competing processes of self-focusing and multiphoton ionization/plasma absorption. Below P_{cr}, not enough energy remains, and the plasma column dissipates. A schematic of these focusing-defocusing cycles is depicted in figure 2.

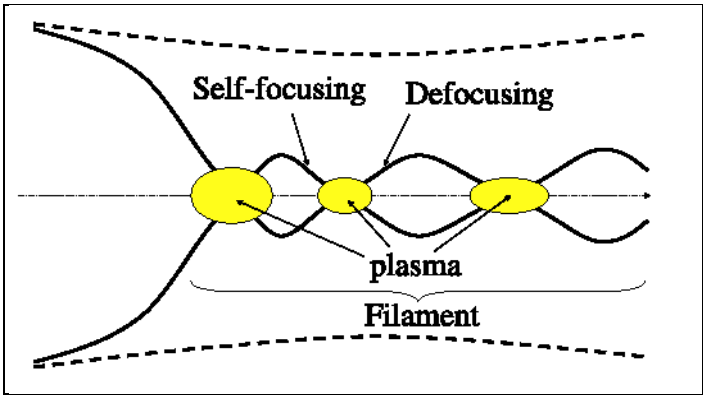

Figure 2. Schematic of beam focusing and defocusing cycles. Solid curves indicate the beam core. The dashed line is the root mean square radius of the beam (*2*).

At peak pulse powers >2 P_{cr}, instability within the beam will result in the formation of multiple filaments, each having a power roughly equal to P_{cr}. As the filaments propagate and power is lost, filaments whose power becomes $<P_{cr}$ terminate, and their remaining energy is returned to the energy reservoir surrounding the filaments. Filament numbers reduce gradually with propagation distance until only one filament remains.

The propagating filament in air produces a broad spectrum of white light (*6*). Figure 3 depicts the spectral properties of the white light supercontinuum as measured by Théberge et al. (*7*).

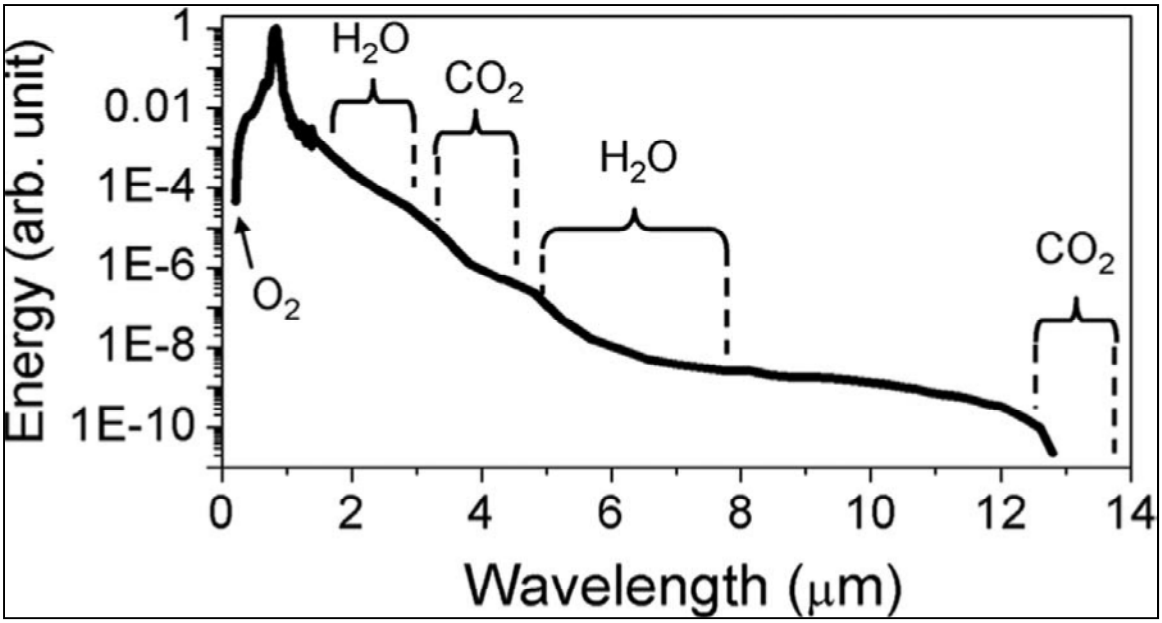

Figure 3. Measured white light spectrum generated by 1.4-TW laser pulses. Dips in the emission spectrum (labeled in the figure) correspond to the absorbance of continuum emission by molecular components of air (*7*).

At the terminus of the propagating filament, the supercontinuum takes the form of a slowly diverging conical emission. In cross section, the emission appears as a central white light surrounded by additional colors appearing as concentric rings surrounding the white core. The color order of the rings is the inverse of conventional diffraction, with blue components of the spectrum appearing in the outer rings. The divergence half-angle of this conic emission is dependent on light frequency and is roughly 0.12° for 500-nm light produced by a Ti:Sapphire laser (*2, 3*).

4. Experimental Studies of Femtosecond Laser Filaments Propagating Through H_2O Aerosols

The earliest experiments demonstrating the interaction of filaments propagating through air and interacting with water droplets were performed by Courvoisier et al. (*13*) in 2003. Using an USPL operating with a pulse energy of 7 mJ/pulse and pulse duration of 120 fs (~58 GW), the authors produced filaments in their laboratory. In these experiments, single droplets of water were placed in the center of the filament at a distance of 1 m from the filament origin. Pulse energy contained within the propagating filament (in the presence and absence of the droplet) was determined by allowing the filament to drill an aperture in foil and then measuring the transmitted energy. Results for a freely propagating (unobscured) filament and a filament propagating after interaction with a 50-μm droplet are shown in figure 4.

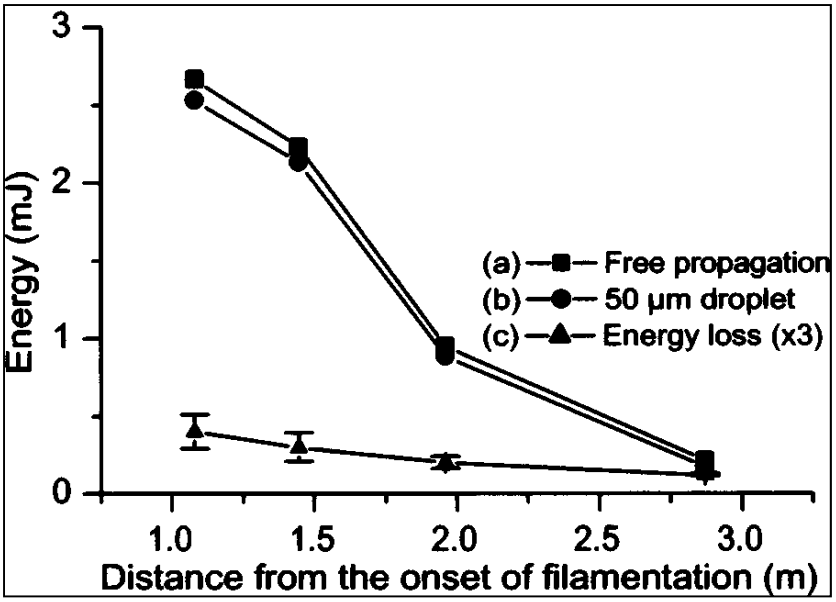

Figure 4. Laser pulse energy contained in (a) a freely propagating filament and (b) a propagating filament after interaction with a 50-μm droplet as a function of the distance after the formation of the filament. The loss of energy due to the interaction (c) with the droplet is magnified by a factor of 3 to aid in viewing (*13*).

Placing a 50-μm droplet in the filament produced little impact on the propagating laser filament. Small energy losses, about 130 μJ, relative to the unobscured filament were observed immediately beyond the filament/droplet interaction, and overall filament energy differed only slightly, about 40 μJ, relative to a freely propagating beam at the filament terminus (3 m from the nonlinear focus). A decrease in the pulse energy difference between the freely propagating and obscured filaments (curve c) led Courvoisier et al. to conclude that energy in the obscured filament was being replenished by the surrounding energy reservoir and is consistent with earlier studies which demonstrated that blocking the filament energy reservoir results in a loss of continued filament propagation (*21*). Propagation of the filament beyond single droplets was further demonstrated for transparent and absorbing (dyed with ink) droplets with sizes up to 95 μm (64% obstruction of a typical 150-μm filament). In this instance, reported energy losses in the filament immediately after the large 95-μm droplets were about 300–400 μJ.

In addition to investigating the effects of single droplets, the authors investigated the effect of droplet distributions on filament propagation. Filaments were propagated through a 0.35-m open cloud chamber, and the transmitted energy measured. Filament propagation was studied in this chamber for several optical thicknesses, τ. At low optical thickness values ($\tau = 1.2$), full transmittance of the filament was observed. Propagation of the filament through the chamber was demonstrated for values of optical thickness as high as 3.2; however, once the beam entered unobstructed air beyond the chamber, propagation of the filament terminated due to energy losses in the energy reservoir required for replenishment. The authors also observed that the

exponential decay of filament transmission with droplet concentration was consistent with linear scattering, indicating that depletion of the energy reservoir is dominated by Mie scattering processes.

In experiments performed by Bochkarev et al. (*22*) comparing optical transmission of ultrashort laser pulses and continuous wave (CW) laser emission in the presence of water aerosols, they observed a similar decay in optical transmission. Ultrashort laser pulses (λ_0 = 800 nm, pulse energy = 17 mJ, τ_p = 80 fs) and CW laser emission (λ_0 = 630 nm) were passed through a jet of water droplets with a root mean square radius of ~2.5 μm and particle concentration $<10^7$ cm^{-3}. Transmission of the filamented laser pulses was observed to adhere to Bouguer's law (sometimes referred to as the Beer-Lambert or Beer-Lambert-Bouguer law) (*23*), i.e., the transmission decreased exponentially, while the aerosolized particle concentration increased (figure 5). A comparison of extinction coefficients predicted by Bouguer's law for 800-nm CW laser emission (dashed line) with 800-nm femtosecond pulses indicated a slightly higher extinction coefficient (~35% higher) for the femtosecond pulses. The authors attributed this difference to a loss in laser energy resulting from multiphoton ionization processes that occur as the ultrashort pulse propagates through air.

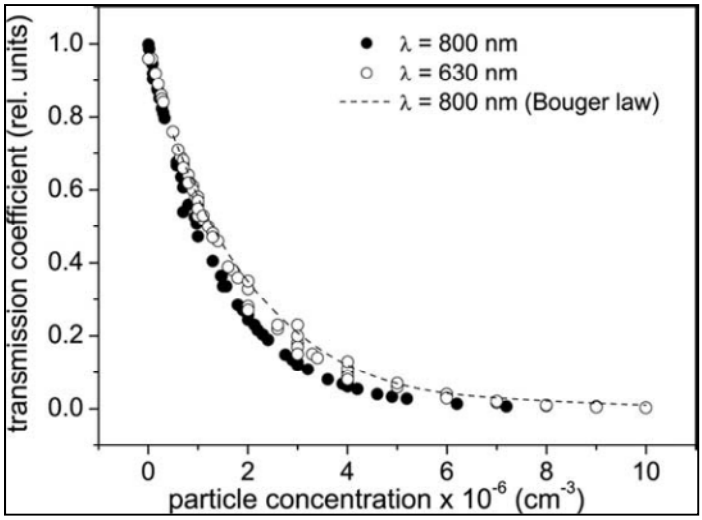

Figure 5. Optical transmission of water aerosol at two wavelengths vs. particle concentration. Theoretical transmission of 800 nm predicted by Bouguer's law is indicated by a dotted line (*22*).

Ackermann et al. (*24*) experimented with filaments in rain-like conditions as part of a study aimed at understanding the use of filaments for triggering lightning discharges. Filaments produced by an USPL system were propagated across a 1.2-m gap through a droplet spray generated between two electrodes at a fixed voltage of 1050 kV. The consistency of the spray was equivalent to heavy rain (1.4 mm/min, mean droplet diameter 0.5 mm, droplet density of 0.3 droplets/cm^3). Survival of the propagating filaments was confirmed by inspecting the laser beam profile at the electrode surface. Triggering of voltage discharge was observed for laser

pulse energies as low as 60 mJ (τ_p = 170 fs), with an increased probability of discharge through a cloud observed at higher pulse energies. Upon completing this work, the authors demonstrated that filaments could be used as an electrical conduction path to trigger and guide high-voltage discharges in conditions equivalent to a dense cloud.

In addition to these laboratory studies, filamentation through aerosols and water droplets has been investigated using relevant atmospheric propagation scales. Using the Teramobile laser system (*9*), Méjean et al. (*15*) propagated femtosecond laser pulses through 40 m of free air space (at sea level) and into a 10-m-long open cloud chamber. The laser chirp was adjusted (t_p = 600 fs) so filament formation occurred prior to the beam's entry into the cloud (1 μm mean droplet radius, droplet density 6.7×10^4 droplets/cm^3). The minimum laser power required to transmit single filaments through the cloud was ~28 GW (~9 P_{cr}). Higher laser power resulted in the transmission of multiple filaments. For 220-mJ pulses, the residual beam energy after transmission was ~25 mJ/pulse or 45 GW.

Experiments performed by recording beam profiles at the exit of a cloud (50% transmission) chamber for two different incident laser energies, 220 and 90 mJ/pulse (123 P_{cr} and 51 P_{cr}, respectively), demonstrated that beam energy influences the distribution and number of filaments transmitted through the cloud chamber. Propagation through the cloud resulted in about a 50% loss in the number of filaments, e.g., for 123 P_{cr}, only 13 filaments were observed after the cloud chamber compared to 24 observed for free atmospheric propagation. The authors indicated that this behavior is consistent with the cloud acting as a linear power attenuator on the entire beam, removing energy from both the transiting plasma columns and the power reservoir that supports them. Furthermore, the authors concluded that because the clouds did not disrupt the filament transmission, useful filament properties, such as white light generation, are attainable within and beyond aerosol fields in outdoor settings as long as the density of the aerosol cloud permits transmission of several critical powers.

In a second outdoor study, Méchain et al. (*15*) used the Teramobile system to examine the effects of actual rain conditions on the propagation of filaments (*25*). Laser output from Teramobile was propagated at a 3230-m altitude for 150 m through drizzle composed of small droplets (<0.5 mm in size) falling at a rate of several millimeters per hour. Visibility through this drizzle was estimated at 37% transmission over the 150-m distance. Unlike the experiments by Courvoisier and Méjean, where filaments were formed prior to entering a cloud chamber, energy from the laser encountered the drizzle before and after filament formation. Light scattering from the rain did not affect the ability of the ultrashort pulses to self-focus. Furthermore, the authors observed that losses in intensity caused by light scattering off the droplets could provide nucleation centers for the formation of new filaments, and the formation of new filaments compensated for losses of laser energy due to diffraction of the beam. Filaments produced in the drizzle behaved similarly to the previously described laboratory and outdoor studies, i.e., disruption and subsequent replenishment from the energy reservoir resulted in the survival of filaments but at reduced filament numbers compared to propagation through the atmosphere.

5. Theoretical Studies of Femtosecond Laser Filaments Propagating Through H_2O Aerosols

5.1 Simulation of Filament Interaction With Individual Aerosol Droplets

In addition to experimental studies that have demonstrated the survival of filaments through aqueous aerosols in laboratory environments and outdoor settings, theoretical studies have been performed to refine the understanding of how the filament propagates through and interacts with aerosol droplets. Shortly following Courvoisier's work demonstrating the survival of a filament after individual water and ink droplets up to 95 μm in diameter (*13*), several modeling efforts were performed to test the validity of Courvoisier's observations and understand the physical processes behind them.

In the first of these studies, Kolesik et al. (*26*) simulated the filament/aerosol interaction using a femtosecond pulse propagation model that simulates multiple physical processes including diffraction, self-focusing, stimulated Raman scattering, plasma generation, and the interaction of the laser pulse with the plasma. A 50-μm-diameter aerosol droplet, modeled as an opaque screen, was placed at two test locations in a simulated filament propagating over 3 m long (7-mJ pulse energy, τ_p = 140 fs). Placement of this opaque screen at distances of 0.4 and 1.0 m after initiating the filament failed to dissipate the filament. Interaction of the filament with the "droplet" resulted in an immediate loss of several percent of the pulse energy. Rates of energy loss (mJ/m) for a freely propagating filament and perturbed filament remained almost the same, indicating that diffraction caused by the screen is not propagated outside of the beam and is instead captured by self-focusing of the laser pulse. The authors used a simulation of the transverse laser fluence made at the "droplet" and 0.1 m beyond the droplet to demonstrate that healing of the filament results from diffraction and expulsion of light from the off-axis plasma regions of the filament.

In a second work authored at nearly the same time, Skupin et al. (*27*) proceeded to develop two- (2-D) and three-dimensional (3-D) simulations to investigate the reformation of a filament after aerosols. A simulation was performed using propagation equations consisting of an extended nonlinear Schrödinger equation coupled to a Drüde model to account for both the electric field envelope and local plasma density of the propagating laser pulse. Specific parameters used in the simulation may be found in the referenced source. The resulting 3-D simulation reproduced a propagating plasma column with a diameter of 160 μm at a distance of 0.39 m containing ~38% of the input energy, with the remaining energy relegated away from the plasma core. Simulated droplets (50 to 95 μm) were placed in the plane perpendicular to the propagating filament. The filament was reformed within 2 cm of the interaction. Approximate 2-D models were investigated to further understand the replenishment process. In these models, the filament is modeled without a surrounding photon bath of copropagating laser radiation.

Despite the lack of photon reservoir in the simulation, the authors demonstrated that filaments could be rebuilt after interacting with single droplets up to 150–180 μm. The authors concluded that reformation of the filament resulted from a low-power state (after the interaction) undergoing Kerr recompression, with the surrounding photon reservoir playing only a minor role.

5.2 Simulation of Filament Interaction With Multiple Aerosol Droplets

Models of filaments interacting with single droplets, like those of Kolesik (*26*) and Skupin (*27*) described previously, were not detailed enough to simulate realistic scenarios of USPL energy interacting with multiple heterogeneous-sized droplets, such as rain or fog. While these single-droplet models had been focused primarily on reproducing experimental observations, such as self-healing of filaments, expansion on these models was required to elucidate more details about filament formation and interaction with water-based aerosols. In addition to the attenuation of laser power by aerosols, information sought included the effects of laser power, power contained in the filament, aerosol droplet size, droplet density, and aerosol layer thickness on distance before filamentation formation, filament length, and the number and distribution of filaments.

Also of interest was trying to elucidate the origin of filament self-healing or the origination of new filaments after aerosol interaction with the laser pulse. The previous models used by Kolesik and Skupin indicated filament reformation originated from energy dispersed from the filament core or the surrounding plasma periphery. Because their models were designed to examine only single filaments (modeled as solitons) interacting with single droplets, they lacked sufficient detail to describe the potential roles other parts of the laser pulse, such as the photon reservoir, might play in filament formation, self-healing, and propagation in the presence of multiple aerosol droplets.

5.2.1 Continuous Linear Damping as a Model for Multiple Aerosol Droplets in Simulations

Adapting previously developed physical filament propagation models (*28, 29*), Méjean et al. (*15*) simulated filament power attenuation over a distance of 10 m using a linear damping term or randomly generated distribution droplets. In this simulation, a Gaussian beam with a pulse duration of 600 fs and 110 P_{cr} was propagated 1 m before entering a 10-m attenuation region. In the first case, linear damping was applied by setting the linear extinction coefficient ε (see equation 1 in Méjean et al. [*15*]) to a value of 0.07 m^{-1} to produce an attenuation rate of 50% over the 10 m. In the case of random droplets, ε for the aerosol region was determined according to the following expression:

$$\varepsilon = N\pi R^2 , \tag{2}$$

where N is the droplet density, and R is the droplet radius. Equation 2 assumes that the number of droplets in a given distance step along the laser path and at a fixed droplet density can be defined by the Poisson density function, and that individual droplets do not overlap.

Using this model, Méjean et al. demonstrated that filamentation patterns produced after 4 m of propagation using the linearly dampened expression were qualitatively similar to those produced using simulated fields of 25- and 50-μm random droplets. The effect of droplet radii (R) on laser power attenuation was identical, provided the droplet density (N) was adjusted so that the product $N \times R^2$ in equation 2 was held constant. Observations made at a distance of 10 m of propagation indicated that the similarity between the attenuation of laser power by linear damping and by random droplet collisions was maintained. The authors did note, however, that large distance attenuation from the random droplets reached ~55% compared to the fixed simulation with linear damping (fixed at 50%).

Using this linear damping approximation, Méjean et al. (*15*) proceeded to simulate the filament patterns created by a USPL beam freely propagating a distance of 50 m and also for a distance of 40 m followed by 10 m of a dense fog (50% transmission) as a comparison to their previous experimental studies using the Teramobile. In addition, several laser pulse powers were investigated. Simulations performed at a pulse energy of 220 mJ (123 P_{cr}) produced 25 filaments over 50 m of free propagation and 12–15 filaments through the fog (40 m free + 10 m fog). At a pulse energy of 90 mJ (51 P_{cr}), 12 filaments were produced in free propagation and 6 through the fog. The authors concluded that each filament contained ~5 P_{cr} regardless of propagation through free space or through aerosols, and that linear damping losses could be used to simulate energy losses in a propagating filament due to micrometric droplets. Furthermore, the authors mentioned that because clouds have little effect on filamentation and reduce only the number of propagating filaments, desirable features of filamentation, such as white light generation, are possible within clouds as long as the several P_{cr} can be transmitted.

Zemlyanov and Geints (*30*) performed simulations of filaments designed to clarify the impact of water aerosols on the evolution of the filament. Filaments were created using a combination of a nonlinear Schrödinger equation for the varying electronic field envelope coupled to a Drüde plasma model and were simulated in 3-D+1 dimensional space. Attenuating aerosol layers of varying optical thickness were generated in a similar fashion to the previously mentioned work by Méjean et al. (*15*)—i.e., through insertion of a linear extinction term in the filament model—and were placed at various locations along the axis of the simulated propagating laser beam.

Aerosol screens with optical depth of unity ($\varepsilon = 2.27\ m^{-1}$) were placed before and after the nonlinear focus of a filament produced from a laser with the following parameters: λ_0 = 800 nm, τ_p = 80 fs, pulse energy = 8 mJ, $P = 15\ P_{cr}$. Results of these 2-D simulations are shown in figure 6.

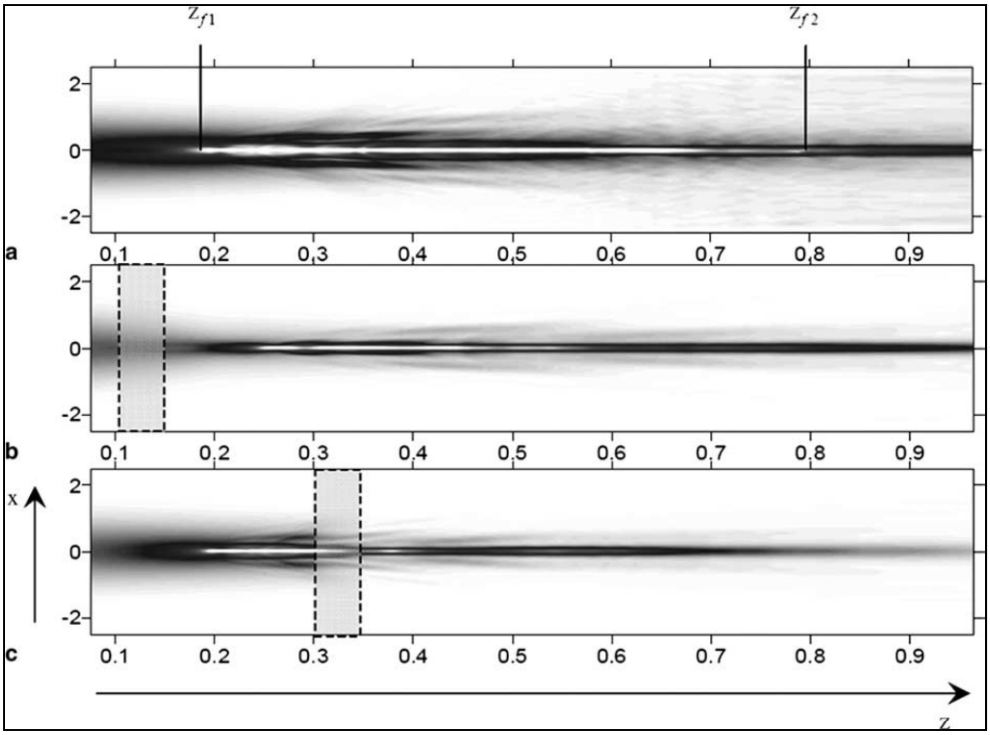

Figure 6. The 2-D fluence profile of propagating filaments (*30*).

Note: Panels A, B, and C represent filament propagation in free atmosphere, propagation with an aerosol screen placed prior to the nonlinear focus, and propagation with an aerosol screen placed after the nonlinear focus, respectively. The axis, *z*, represents normalized distance along the beam path, and the position of the aerosol layer along *z* is indicated by the dashed box.

Placement of the aerosol screen prior to the nonlinear focus shifted the focus (and initiation of the filament, indicated by z_{f1} in the figure) to a larger distance while shortening the filament length ($z_{f2} - z_{f1}$) because of losses to the peak power of the beam, *P*, and losses in stability due to influx of energy from the beam periphery to its core.

When placed after the nonlinear focus (beam already filamented), the filament appeared to be blocked by the aerosol screen. An aerosol attenuation layer five times shorter ($\varepsilon = 11.36\ m^{-1}$) was applied at the same location beyond the nonlinear focus to elucidate the role of a thinner aerosol field. In simulation with this thinner layer, the filament reformed and evolved similar to a freely propagating filament; however, the filament suffered a loss in stability. From these results, the authors concluded that when a filament contacts thick aerosol layers, the longer attenuating optical path gradually reduces filament power by disrupting the balance between Kerr self-focusing and diffraction of the beam, lowering energy replenishment of the core filament from the photon reservoir. This loss of power leads to greater beam diffraction, increased beam cross section, and reduced intensity. This observation contrasts the conclusions made by Kolesik and Skupin that the photon reservoir had little role in reforming the filament after it interacted with aerosols (*26, 27*). Thin attenuating aerosols allow the filament to recover quickly if the beam power is sufficiently high enough above the critical power for filamentation.

5.2.2 Filamentation Modeling Using the Stratified Model for Laser Propagation

More recently, scientists have investigated the simulation of filamentation using models that account for forward light scattering from droplets sized larger than the wavelength of radiation. Prior models had adopted the approach of modeling aerosols as a region of linear attenuation and did not include effects from coherently scattered light. These earlier experimental studies, performed at high particle concentrations (10^6 cm^{-3}), demonstrated minimal nonlinear laser interaction effects with aerosols and instead indicated a linear decrease in pulse energy consistent with Bouguer's law (*13*). Méchain et al. (*25*) followed Courvoisier's experimental work with the previously discussed experiments and theoretical simulations that demonstrated the utility of modeling aerosol regions using linear attenuation fields as a substitute for the random distribution of disks; however, the authors did note some disparity in using linear attenuation fields and disks at longer distances. Recent results obtained by Silaeva and Kandidov (*31*) demonstrate that linear attenuation media cannot account for continued energy losses beyond the aerosol layer, resulting from perturbations by scatter within the aerosol. They concluded that attenuation layers are suitable for describing energy distributions within only the aerosols, not for pulses propagated beyond them.

Prior to the previously mentioned work by Silaeva and Kandidov (*31*), Militsin et al. (*32*) developed the stratified model for laser propagation while exploring different ways to understand ultrashort laser pulse propagation. Unlike the continuous linear attenuating model for aerosols, the stratified model for laser propagation was developed to capture the effects of coherent light scattering forward off particles on the formation, evolution, and propagation of filaments. In the stratified model, USPL radiation is propagated through a series of screens that individually isolate physical components of the propagation. Screens simulating the aerosol portion of the interaction consist of randomly distributed droplets that cause the simulated pulse to coherently scatter in the forward direction; backscattering is considered negligible, as the scattering bodies are much larger than the wavelength of light. Additional screens may be used to simulate nonlinear optical effects (e.g., self-focusing and plasma effects) and linear diffraction. Ensembles of these screens stacked together capture the cumulative effects of aerosol forward scattering, nonlinear interaction with air and plasma, and linear diffraction on the propagating pulse. More specific details on the construction and use of the stratified model, such as the mathematical expressions used in the model and the various variables and parameters required for its use, may be found in Militsin et al. (*17*) and Kandidov and Silaeva (*33*).

In one of the earliest investigations using the stratified model, Kandidov and Militsin (*34*) simulated USPL propagation through rain conditions similar to the previously described experiments of Méchain et al. (*25*). In these simulations, Kandidov and Militsin were able to produce intensity distributions in the laser pulse that were qualitatively similar to those produced in the experiment. Regional areas of high intensity were observed in the simulated cross section of the intensity distribution. The authors attribute the origin of these regions of high intensity to perturbations that have intensified into filament initiation sites through self-focusing.

In a later work, Militsin et al. (*17*) conducted a series of simulations using the stratified model approach to develop a more complete understanding of how the size of water aerosols and the laser power impact the generation of filaments. First, ultrashort laser pulses were simulated propagating through 15 cm of aerosol (N = 10 cm^{-3}), and the increase of intensity due to self-focusing was monitored as a function of propagation distance, particle size, and initial laser power. Results from this simulation are shown in figure 7.

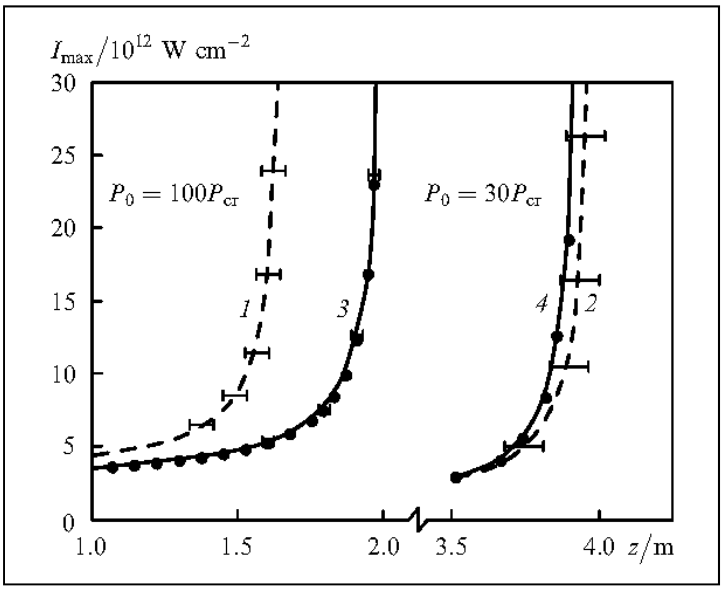

Figure 7. Dependence of maximum laser intensity (I_{max}) on ultra short pulses with peak powers of 100 P_{cr} (P = 600 GW) and 30 P_{cr} (P = 180 GW) on propagation distance (z) and particle radius (r = 15 µm, curves 1 and 2; r = 2 µm, curves 3 and 4) (*17*).

At the small particle radius (curves 3 and 4), the intensity increase due to Kerr self-focusing differed only slightly from free propagation (●) through atmosphere, regardless of the power contained in the pulse. Increasing the power in the pulse from 30 to 100 P_{cr} (180 to 600 GW) shortened the distance to maximal intensity. The rise to maximal intensity was fastest for pulses interacting with the 15-µm aerosols at high pulse power (curve 1); large particles at low power (curve 2) exhibited little difference in trend from free propagation occurring at a similar power. The authors ascribed these observations to perturbations produced by scattering off of the large particles producing spatial instability and nonlinear focusing. At lower laser powers, perturbations from the large aerosols are less significant, resulting in the observed similarities with free propagation and propagation through small aerosols (curves 2 and 4).

Second, Militsin et al. (*17*) investigated the influence of aerosol particle density (N) on distance to maximum intensity. Simulations were performed for aerosol densities ranging from 100 to 1300 cm^{-3} (power, P = 50 P_{cr} or 300 GW; aerosol radius, r = 15 µm). Increasing the particle

density increased the distance to filamentation; above 1100 cm^{-3}, scattering losses exceeded Kerr self-focusing, and filamentation did not occur.

Last, Militsin et al. investigated the influence of aerosol particle density and size on observed filament number. An example of filamentation regime boundaries as a function of aerosol density and size simulated at $P = 50\ P_{cr}$ is shown in figure 8.

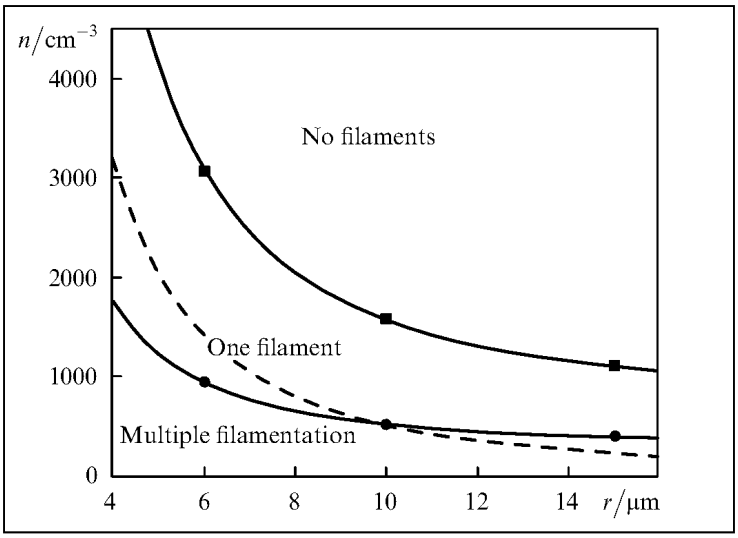

Figure 8. Aerosol size and radius influence on filamentation boundaries, simulated at 50 P_{cr} (P = 300 GW). Solid curves represent simulated data; the dashed curve represents a constant extinction coefficient ($\varepsilon = 0.32\ m^{-1}$) (*17*).

This simulation showed that filamentation performed at constant extinction can result in a change from single to multiple filamentation depending on aerosol size and density. From this, Militsin concluded that interaction with the aerosol can not only attenuate the intensity of the laser pulse, but also induce instability, leading to multiple filament generation.

The studies performed by Militisin and others investigated only monodisperse aerosols. Kachan and Militsin (*16*) expanded on these previous works by simulating filament propagation through aerosol distributions representative of authentic atmospheric aerosols. Ultrashort laser pulses propagating through polydisperse aerosols were simulated using the stratified model. The average particle radius was 4 μm, and the distribution was generated using a generalized gamma distribution ($N = 100\ cm^{-3}$, $\varepsilon = 16.7\ km^{-1}$). An example of the intensity profile in the plane of the laser cross section at 2 m for a polydisperse aerosol is shown in figure 9.

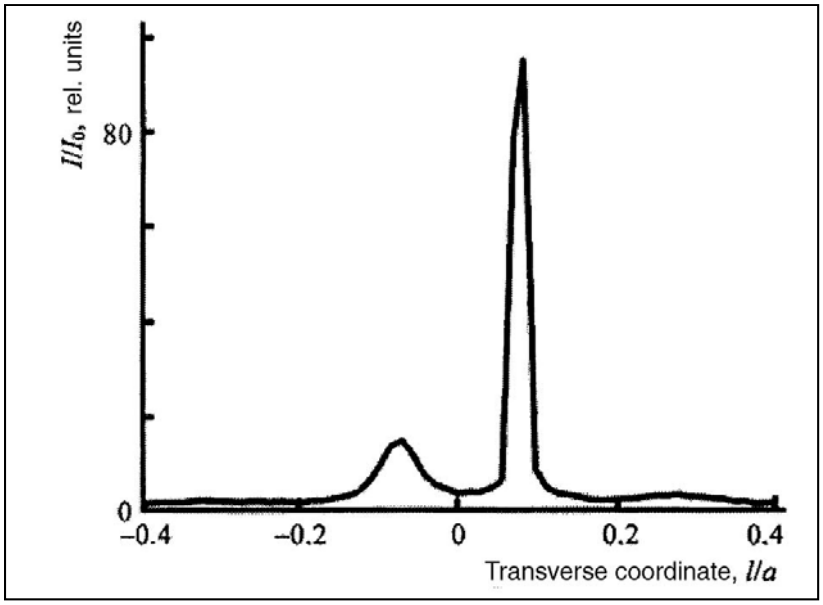

Figure 9. Transverse intensity profile of a USPL beam propagating through a polydiserse aerosol at a distance of 2 m (*16*).

Despite the presence of the polydisperse aerosol, intensity maxima exceeding the initial peak intensity are formed by Kerr self-focusing (indicated by peaks in the figure). Under typical conditions necessary for filamentation, these maxima are expected to produce filaments.

When simulations were carried out using the same polydisperse aerosol at several different droplet densities (20, 100, and 500 cm^{-3}) and constant peak power ($P = 100\ P_{cr}$ or 600 GW), the number of filaments produced in the propagating beam increased slightly with an increase in droplet density. A decrease in the distance to which the filaments formed was also observed.

5.2.3 Filament Propagation Under the Cumulative Effects of Turbulence and Aerosols Modeled by the Stratified Model

Of further interest to the propagation of ultrashort laser pulses through obscurants is the additive effect of turbulence. Experiments investigating the influence of turbulence on propagating filaments have demonstrated that filaments can survive localized turbulence up to five times the magnitude of typical atmospheric conditions (*35*). More recently, Salamé et al. (*36*) investigated 1.3-m-long turbulence regions swept along the propagation axis of a USPL beam. The authors noted a decrease in the number of filaments that survive the turbulence but observed no effect on the spectral properties of filaments, including processes such as self-phase modulation and third harmonic generation. Furthermore, the authors indicated that scaling of these laboratory results suggests typical atmospheric turbulence will have little effect over kilometer ranges. It should be noted that this view is not equally shared in the USPL user community. The authors admit that "such large-scale extrapolation from laboratory-scale data may be hazardous" (*36*) and that further research into the effects of turbulence to increase the understanding of its effects on USPL propagation may be merited.

Silaeva et al. (*18*) performed simulations of USPL propagation through the combined effects of aerosol and turbulence. Prior to the simulations discussed in the work, the authors noted several other studies (see references contained within) with results contrary to the observations of Salamé et al. (*36*). These additional studies include observations that filament properties in the presence of turbulence, such as distance to filamentation, are highly dependent on turbulence conditions and laser peak power, and present experimental evidence of turbulence-driven modulation instability development within the ultrashort laser pulse.

Simulations of filamentation in the presence of turbulence and aerosols were performed at P = 50 P_{cr} (200 GW) (*18*). Aerosol screens consisted of particles with a radius of 15 µm and particle density of 10 cm^{-3}. Turbulence was modeled using a modified von Kármán spectrum (*37*) expanded into a 2-D screen with the following parameters: refractive index structure constant $C_n^2 = 10^{-13}$ $cm^{-2/3}$; inner scale of turbulence l_0 = 1 mm; and outer scale of turbulence L_0 = 1 m (figure 10).

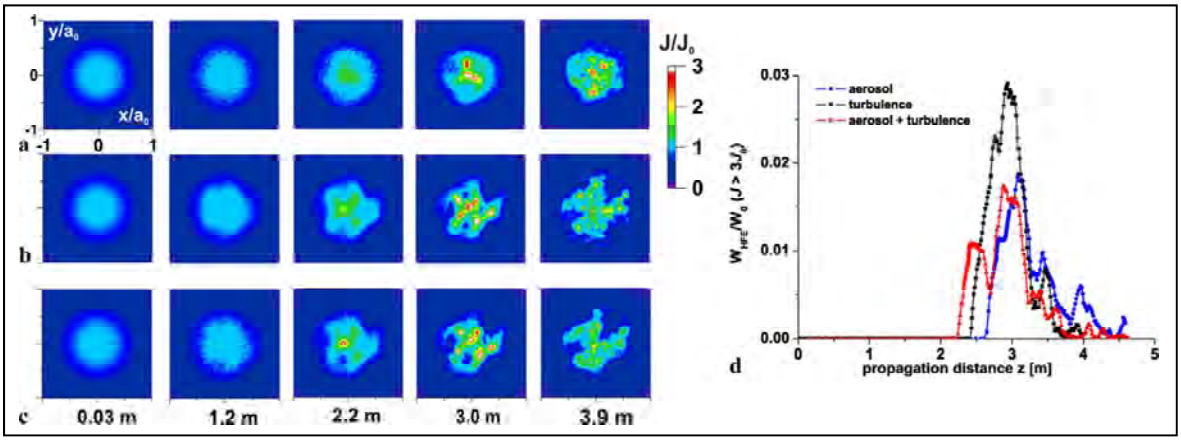

Figure 10. Fluence distribution of USPL at different distances (a) in aerosol, (b) in turbulent atmosphere, and (c) in both turbulence and aerosol. The influence of pulse energy as a function of propagation distance is shown in (d) (*18*).

From these simulations, the authors assembled an overall view of the laser/turbulence/aerosol interaction. Turbulence and aerosols both resulted in perturbations of the light field. In the presence of aerosol only (figure 10[a]), small-scale perturbations in the laser fluence distribution due to laser scattering on discrete droplets are immediately visible as small diffraction rings. At longer distances (1.2–2.2 m), the aerosol interaction appears as a speckle pattern in the beam cross section. The formation of filaments (indicated by areas of high intensity) is delayed slightly relative to the filaments produced when only turbulence is present. Turbulence-induced perturbations (figure 10[b]) were visible in the fluence distributions only near the start of filamentation (2.2 m). Initial filamentation sites, such as the region of high intensity seen at 2.2 m, are redistributed into multiple areas of high intensity by the turbulence, resulting in more filaments than observed in aerosol propagation at similar propagation distances. The combination of the two processes (figure 10[c]) results in a combination of the two effects.

Small-scale perturbations are observed early in the propagation, and regions of high intensity begin to form. Effects from turbulence then redistribute the energy within the pulse, forming new high-intensity regions (i.e., sources of filamentation).

Analysis of the pulse energy (figure 10[d]) indicates that aerosol scattering produces greater decreases in pulse energy than turbulence, and that aerosol scattering is the dominant cause for pulse energy reduction when both aerosol and turbulence effects are present. Additionally, Silaeva et al. (*18*) showed that for a filament forming in turbulence, the addition of aerosols delayed the start distance for forming the filament. The authors attribute this behavior to aerosol scattering slowing down filamentation by reducing pulse energy, while simultaneously initiating filaments by providing filamentation sites resulting from the coherent scattering of the laser radiation.

6. Propagation Through Obscurants on the Battlefield

The battlefield environment represents a worst-case scenario for laser propagation providing for substantial losses to laser energy even over short distances. In addition to atmospheric water vapor and dust, other heterogeneous particle sources may be present, such as diesel exhaust, miscellaneous combustion by-products and man-made smokes (*38*). Before USPLs will be useful on the battlefield, further experimentation and simulation is required to develop a fundamental understanding of how the "known" properties of filament formation and propagation will translate to this significantly more complex environment. Specifically, progress needs to be made in several areas of fundamental science discussed in the following sections.

6.1 Interaction of Filaments With Complex Aerosols and Obscurants

The propagation of ultrashort laser pulses and filaments has only been investigated in aerosols composed of liquid water. The spectral properties of water are well known, and water aerosols are composed of well-defined spheres of a fixed size or distribution. In contrast, the battlefield aerosol may be of mixed composition, having shapes ranging from grains as seen in soils and dusts to smooth particles of carbon present in explosive detonation plumes. These aerosols likely exhibit a nonuniform size distribution and have vastly different spectral characteristics than water. In addition, the composition and density of these aerosols can rapidly change, e.g., large particles will quickly settle out of a detonation occurring on soil and smaller particles may persist in the air for hours, drifting along with changing wind currents (*38*). The physical nature of the laser/aerosol interaction may also vary greatly with laser-operating parameters, such as laser wavelength, power, spectral chirp, and pulse duration.

6.2 Instrumental Factors Necessary To Achieve Desired Light Delivery on Target

Closely related to the need to understand how the propagation of laser pulses and filaments is affected by complex aerosols is the need to understand how to "tweak" the laser parameters to reliably propagate the laser energy in the presence of any complex aerosol and to affect the target in a desired fashion. Propagation of ultrashort laser pulses and the generation of filaments in air can be manipulated by adjustments in laser wavelength, pulse duration, and placement of the nonlinear focus. Turbulence along the laser path will also affect the pulse propagation, especially when coupled with effects arising from aerosol interactions.

6.3 Understanding Limitations and Advantages of Ultrashort Pulsed Laser Propagation so That USPLs Can Be Used to Greatest Effect on the Battlefield

While experiments and simulations are developed to determine the influence of complex aerosols and optimal operating parameters, careful consideration must be made into how these phenomena can best be utilized for the Soldier. USPLs may play a role in the battlefield from guidance to target designation to optical damage and sensing. However, the constraints imposed by the physics of propagation must be considered. For example, the physics governing laser power attenuation due to scattering and absorbance will occur regardless of the laser pulse duration, intensity, and nonlinear effects. A laser sensing application may be able to deliver radiation to the target, but getting information back through the scattering/absorbing medium remains a challenge that will still have to be addressed. Understanding these and other details is required for successful development and application of USPLs in the battlefield.

7. Conclusions

Researchers have conducted experimental studies both in laboratories and in the outdoors demonstrating the survival or reformation of single and multiple laser filaments in air after interaction with single water droplets, droplet distributions, and rain. The influence of aerosol size, droplet density, and aerosol layer thickness on the residual laser power and numbers of surviving filaments has also been investigated. Theoretical simulations have been undertaken to gain greater insight into the physical processes observed in these experiments. The use of filamentation models, such as the stratified model for filament propagation, shows that the distance to filament formation and length varies with the nonlinear focus of the laser pulse, aerosol particle size, and laser power. Furthermore, these models have been used to broaden the understanding of the role of coherent light scatter in forming filaments following interruption by aerosolized media.

The propagation of ultrashort laser pulses and the formation and propagation of laser filaments in the battlefield environment present a more complex problem. Aerosols in this environment will exhibit vastly different physical properties (shape, size, composition) than the water-based

aerosols presently discussed in current literature sources. Little or no work on the interaction of ultrashort laser pulses with battlefield particulates has been documented. Consequently, complex studies need to be performed to understand how these aerosols will impact a propagating laser pulse or filament. Final application in a battlefield environment will require an understanding of the role of laser parameters (e.g., laser power, wavelength, and pulse duration) and atmospheric propagation parameters (e.g., existing aerosol composition/size/morphology, aerosol thickness, turbulence, and range to target) necessary to place laser pulses and filaments at desired locations under the prevailing conditions. A definition of this parameter space will require further experimentation under many conditions and the development of more detailed simulation and predictive models.

The use of USPL systems in the battlefield environment represents a distant but realizable goal. In addition to understanding the interaction of ultrashort laser pulses and filaments with complex aerosols and particulates, much fundamental research and understanding is still required in the area of the formation and propagation of laser filaments in air. Many unanswered questions remain. For example, what are the exact physical processes behind filament formation and replenishment? Experimental evidence supports the reservoir description made in section 3 of this work. In contrast, models of filaments using only solitons (i.e., no energy reservoir) still result in filament formation and propagation in air. Other areas of debate include the plasma nature of the filament (Is it a plasma or is the atmosphere only weakly ionized?) and the amount of laser power contained in an individual filament (3–10 GW). For filaments interacting with aerosols, does the reformed filament retain any of the characteristics of a parent filament?

Future investigative efforts at the U.S. Army Research Laboratory are aimed at addressing some of these fundamental scientific questions while keeping to the distant goal of battlefield application of USPLs and filaments. Planned experiments include the following:

- Developing diagnostic methods for measuring the refractive index of the filament under various operating parameters to help elucidate the role these parameters have upon the filament formation and propagation.
- Studying target effects to understand how laser parameters influence the interaction of the filament with various target materials.
- Studying aerosols to characterize battlefield particulates and their impact on filament formation and propagation.

8. References

1. Braun, A.; Korn, G.; Liu, X.; Du, D.; Squier, J.; Mourou, G. Self-Channeling of High-Peak-Power Femtosecond Laser Pulses in Air. *Opt. Lett.* **1995**, *20* (1), 73–75.

2. Couairon, A.; Mysyrowicz, A. Femtosecond Filamentation in Transparent Media. *Phys. Rep.* **2007**, *441*, 47–189.

3. Kandidov, V. P.; Shlenov, S. A.; Kosareva, O. G. Filamentation of High-Power Femtosecond Laser Radiation. *Quantum Electron.* **2009**, *39* (3), 205–228.

4. Bergé, L.; Skupin, S.; Nuter, R.; Kasparian, J.; Wolf, J. P. Ultrashort Filaments of Light in Weakly Ionized, Optically Transparent Media. *Rep. Prog. Phys.* **2007**, *70*, 1633–1713.

5. Méchain, G.; D'Amico, C.; Andre, Y. B.; Tzortzakis, S.; Franco, M.; Prade, B.; Mysyrowicz, A.; Couairon, A.; Salmon, E.; Sauerbrey, R. Length of Plasma Filaments Created in Air by a Multiterawatt Femtosecond Laser. *Opt. Commun.* **2005,** *247*, 171–180.

6. Kasparian, J.; Sauerbrey, R.; Mondelain, D.; Niedermeier, S.; Yu, J.; Wolf, J. P.; Andre, Y. B.; Franco, M.; Prade, B.; Tzortzakis, S.; Mysyrowicz, A.; Rodriguez, M.; Wille, H.; Woeste, L. Infrared Extension of the Supercontinuum Generated by Femtosecond Terawatt Laser Pulses Propagating in the Atmosphere. *Opt. Lett.* **2000**, *25* (18), 1397–1399.

7. Théberge, F.; Châteauneuf, M.; Ross, V.; Mathieu, P.; Dubois, J. Ultrabroadband Conical Emission Generated From the Ultraviolet Up to the Far-Infrared During the Optical Filamentation in Air. *Opt. Lett.* **2008**, *33* (21), 2515–2517.

8. Wöste, L.; Frey, S.; Wolf, J.-P. LIDAR-Monitoring of the Air With Femtosecond Plasma Channels. *Adv. At., Mol. Opt. Phys.* **2006**, *53*, 413–441.

9. Wille, H.; Rodriguez, M.; Kasparian, J.; Mondelain, D.; Yu, J.; Mysyrowicz, A.; Sauerbrey, R.; Wolf, J. P.; Wöste, L. Teramobile: A Mobile Femtosecond-Terawatt Laser and Detection System. *Eur. Phys. J. AP* **2002**, *20*, 183–190.

10. Daigle, J.-F.; Mathieu, P.; Roy, G.; Simard, J.-R.; Chin, S. L. Multi-Constituents Detection in Contaminated Aerosol Clouds Using Remote-Filament-Induced Breakdown Spectroscopy. *Opt. Commun.* **2007**, *278*, 147–152.

11. Xu, H. L.; Mejean, G.; Liu, W.; Kamali, Y.; Daigle, J. F.; Azarm, A.; Simard, P. T.; Mathieu, P.; Roy, G.; Simard, J. R.; Chin, S. L. Remote Detection of Similar Biological Materials Using Femtosecond Filament-Induced Breakdown Spectroscopy. *Appl. Phys. B Lasers Opt.* **2007**, *87* (1), 151–156.

12. Mirell, D.; Chalus, O.; Peterson, K.; Diels, J.-C. Remote Sensing of Explosives Using Infrared and Ultraviolet Filaments. *J. Opt. Soc. Am. B* **2008**, *25* (7), B108–B111.

13. Courvoisier, F.; Boutou, V.; Kasparian, J.; Salmon, E.; Méjean, G.; Yu, J.; Wolf, J.-P. Ultraintense Light Filaments Transmitted Through Clouds. *Appl. Phys. Lett.* **2003**, *83* (2), 213–215.

14. Kandidov, V. P.; Militsin, V. O. Intensity of Light Field and Electron Concentration in the Laser-Induced Plasma in a Droplet of Water Aerosol Exposed to a Femtosecond Laser Pulse. Geometric Optics Analysis. *Atmos. Oceanic Opt.* **2004,** *17* (1), 46–53.

15. Méjean, G.; Kasparian, J.; Yu, J.; Salmon, E.; Frey, S.; Wolf, J. P.; Skupin, S.; Vinçotte, A.; Nuter, R.; Champeaux, S.; Bergé, L. Multifilamentation Transmission Through Fog. *Phys. Rev. E: Stat., Nonlinear, Soft Matter Phys.* **2005**, *72*, 026611.

16. Kachan, E. P.; Militsin, V. O. How the Particles of the Atmospheric Aerosol Affect the Generation of Filaments in a Laser Beam. *J. Opt. Technol.* **2006,** *73* (11), 772–777.

17. Militsin, V. O.; Kachan, E. P.; Kandidov, V. P. Multiple Scattering, Modulation Instability, and Filamentation of a Femtosecond Laser Pulse in a Dispersion Medium. *Quantum Electron.* **2006**, *36* (11), 1032–1038.

18. Silaeva, E. P.; Shlenov, S. A.; Kandidov, V. P. Multifilamentation of High-Power Femtosecond Laser Pulse in Turbulent Atmosphere With Aerosol. *Appl. Phys. B Lasers Opt.* **2010**, *101* (1–2), 393–401.

19. Marburger, J. H. Self-Focusing: Theory. *Prog. Quantum Electron.* **1975**, *4*, 35–110.

20. Liu, W.; Chin, S. L. Direct Measurement of the Critical Power of Femtosecond Ti: Sapphire Laser Pulse in Air. *Opt. Express* **2005**, *13* (15), 5750–5755.

21. Chin, S. L.; Brodeur, A.; Petit, S.; Kosareva, O. G.; Kandidov, V. P. Filamentation and Supercontinuum Generation During the Propagation of Powerful Ultrashort Laser Pulses in Optical Media (White Light Laser). *J. Nonlinear Opt. Phys. Mater.* **1999**, *8*, 121–146.

22. Bochkarev, N. N.; Zemlyanov, A. A.; Zemlyanov, A. A.; Kabanov, A. M.; Kartashov, D. V.; Kirsanov, A. V.; Matvienko, G. G.; Stepanov, A. N. Experimental Investigation Into Interaction Between Femtosecond Laser Pulses and Aerosol. *Atmos. Oceanic Opt.* **2004**, *17*, 861–864.

23. Saleh, B. E. A.; Teich, M. C. *Fundamentals of Photonics*, 2nd ed.; Wiley: New York, 2007.

24. Ackermann, R.; Stelmaszczyk, K.; Rohwetter, P.; Méjean, G.; Salmon, E.; Yu, J.; Kasparian, J.; Méchain, G.; Bergmann, V.; Schaper, S.; Weise, B.; Kumm, T.; Rethmeier, K.; Kalkner, W.; Wöste, L.; Wolf, J. P. Triggering and Guiding of Megavolt Discharges by Laser-Induced Filaments Under Rain Conditions. *Appl. Phys. Lett.* **2004**, *85* (23), 5781–5783.

25. Méchain, G.; Méjean, G.; Ackermann, R.; Rohwetter, P.; Andre, Y. B.; Kasparian, J.; Prade, B.; Stelmaszczyk, K.; Yu, J.; Salmon, E.; Winn, W.; Schlie, L. A.; Mysyrowicz, A.; Sauerbrey, R.; Wöste, L.; Wolf, J. P. Propagation of FS TW Laser Filaments in Adverse Atmospheric Conditions. *Appl. Phys. B: Lasers Opt.* **2005**, *80*, 785–789.

26. Kolesik, M.; Moloney, J. V. Self-Healing Femtosecond Light Filaments. *Opt. Lett.* **2004,** *29* (6), 590–592.

27. Skupin, S.; Bergé, L.; Peschel, U.; Lederer, F. Interaction of Femtosecond Light Filaments With Obscurants in Aerosols. *Phys. Rev. Lett.* **2004**, *93* (2), 023901.

28. Bergé, L.; Skupin, S.; Lederer, F.; Méjean, G.; Yu, J.; Kasparian, J.; Salmon, E.; Wolf, J. P.; Rodriguez, M.; Wöste, L.; Bourayou, R.; Sauerbrey, R. Multiple Filamentation of Terawatt Laser Pulses in Air. *Phys. Rev. Lett.* **2004**, *92*, 225002.

29. Skupin, S.; Bergé, L.; Peschel, U.; Lederer, F.; Méjean, G.; Yu, J.; Kasparian, J.; Salmon, E.; Wolf, J. P.; Rodriguez, M.; Wöste, L.; Bourayou, R.; Sauerbrey, R. Filamentation of Femtosecond Light Pulses in the Air: Turbulent Cells vs. Long-Range Clusters. *Phys. Rev. E: Stat., Nonlinear, Soft Matter Phys.* **2004**, *70*, 046602.

30. Zemlyanov, A. A.; Geints, Y. E. Filamentation Length Of Ultrashort Laser Pulse in Presence of Aerosol Layer. *Opt. Commun.* **2006**, *259* (2), 799–804.

31. Silaeva, E. P.; Kandidov, V. P. Propagation of a High-Power Femtosecond Pulse Filament Through a Layer of Aerosol. *Atmos. Oceanic Opt.* **2009**, *22* (1), 26–34.

32. Militsin, V. O.; Kouzminskii, L. S.; Kandidov, V. P. Beam Breakup and Filament Initiation Induced by Femtosecond Pulse Transmission Through Water Aerosol. *Proc. SPIE-Int. Soc. Opt. Eng.* **2005**, *5708*, 277–287.

33. Kandidov, V. P.; Silaeva, E. P. Self-Focusing and Multiple Filamentation of Laser Light in Disperse Media. *J. Russ. Laser Res.* **2009**, *30* (4), 305–320.

34. Kandidov, V. P.; Militsin, V. O. Computer Simulation of Laser Pulse Filament Generation in Rain. *Appl. Phys. B: Lasers Opt.* **2006**, *83*, 171–174.

35. Ackermann, R.; Méjean, G.; Kasparian, J.; Yu, J.; Salmon, E.; Wolf, J. P. *Opt. Lett.* **2006**, *31*, 86–88.

36. Salamé, R.; Lascoux, N.; Salmon, E.; Ackermann, R.; Kasparian, J.; Wolf, J. P. Propagation of Laser Filaments Through an Extended Turbulent Region. *Appl. Phys. Lett.* **2007**, *91*, 171106.

37. Andrews, L. C.; Phillips, R. L. *Laser Beam Propagation Through Random Media*, 2nd. ed.; SPIE: Bellingham, WA, 2005.

38. Turner, R. E.; Eitner, P. G.; Leonard, C. D.; Snyder, D. G. S. *Battlefield Environment Obscuration Handbook, Volume I*; SAI-80-009-AA; Science Applications, Inc.: Ann Arbor, MI, 1980. Available from the Defense Technical Information Center database, http://handle.dtic.mil/100.2/ADA102822 (accessed 31 October 2011).

INTENTIONALLY LEFT BLANK.

List of Symbols, Abbreviations, and Acronyms

2-D	two dimensional
3-D	three dimensional
C_n^2	index of refraction structure constant function
CW	continuous wave
I_{max}	maximum intensity
n_0	linear refractive index
n_2	nonlinear Kerr index coefficient
N	droplet density
LIDAR	light detection and ranging
l_0	inner scale
L_0	outer scale
P	laser output power
P_{cr}	critical power in a filament
R or r	droplet radius
USPL	ultrashort pulsed laser(s)
ε	linear extinction coefficient (indicated as α in some of the original works referenced herein)
λ_0	laser source wavelength
τ	optical thickness
t_p	laser pulse duration

NO. OF COPIES	ORGANIZATION
1 (PDF only)	DEFENSE TECHNICAL INFORMATION CTR DTIC OCA 8725 JOHN J KINGMAN RD STE 0944 FORT BELVOIR VA 22060-6218
1	DIRECTOR US ARMY RESEARCH LAB IMNE ALC HRR 2800 POWDER MILL RD ADELPHI MD 20783-1197
1	DIRECTOR US ARMY RESEARCH LAB RDRL CIO LL 2800 POWDER MILL RD ADELPHI MD 20783-1197
1	DIRECTOR US ARMY RESEARCH LAB RDRL CIO MT 2800 POWDER MILL RD ADELPHI MD 20783-1197
1	DIRECTOR US ARMY RESEARCH LAB RDRL D 2800 POWDER MILL RD ADELPHI MD 20783-1197

NO. OF COPIES ORGANIZATION

1 ARMY RESEARCH OFFICE
RDRL ROP P
R HAMMOND
BLDG 4300
DURHAM NC 27703

1 ADELPHI LABORATORY CENTER
RDRL SEE
G WOOD
BLDG 207 3D-44
ADELPHI MD 20783-1197

1 ARDEC
AMSRD AAR WSW A
G BADER
BLDG 65
PICATINNY ARSENAL NJ 07806

1 AIRFORCE RESEARCH LABORATORY
AFRL/RDLA
W ROACH
3550 ABERDEEN AVE SE
KIRTLAND AFB NM 87117-5576

1 LAWRENCE BERKLEY NATIONAL LABORATORY (LBL)
R RUSSO
SENIOR SCIENTIST
LASER MATERIALS INTERACTION GROUP
1 CYCLOTRON RD
BERKLEY CA 94720

1 CREOL COLLEGE OF OPTICS & PHOTONICS
M RICHARDSON
4000 CENTRAL FLORIDA BLVD
ORLANDO FL 32816-2368

1 NAVAL RESEARCH LABORATORY
J AUXIER
CODE 5751
4555 OVERLOOK AVE SW
WASHINGTON DC 20375-5339

NO. OF COPIES ORGANIZATION

1 DEPT OF PHYSICS & ASTRONOMY
J C DIELS
UNIV OF NEW MEXICO
800 YALE BLVD NE
ALBUQUERQUE NM 87131

ABERDEEN PROVING GROUND

24 (18 HC 6 CD) DIR USARL
RDRL WM
B FORCH
P PLOSTINS
RDRL WML
J NEWILL
RDRL WML A
F DELUCIA (1 HC, 1 CD)
A MIZIOLEK (1 HC, 1 CD)
C MUNSON (1 HC, 1 CD)
W OBERLE (1HC, 1 CD)
L STROHM
RDRL WML B
J GOTTFRIED (1 HC, 1 CD)
R SAUSA
RDRL WML C
K MCNESBY
RDRL WMP
P BAKER
S SCHOENFELD
RDRL WMP A
B RINGERS
A PORWITZKY
A VALENZUELA (1 HC, 1 CD)
RDRL WMP C
T BJERKE
RDRL WMP G
B HOMAN

INTENTIONALLY LEFT BLANK.